Coupling transformer operation of a dynamic voltage restorer with electronics protected from fault currents under electrical grid conditions

Hervé Roisse, Guillaume Parent, M Rossi, Virginie Majchrzak

Coupling Transformer Operation of a Dynamic Voltage Restorer with Electronics Protected from Fault Currents Under Electrical Grid Conditions

Hervé Roisse, Guillaume Parent, Mathieu Rossi and Virginie Majchrzak
Univ. Artois, EA 4025, Laboratoire Systèmes Électrotechniques et Environnement (LSEE), F-62400 Béthune, France

***Abstract*—To improve electrical grids power quality, a dynamic voltage restorer with a magnetic voltage source converter protection scheme integrated in the coupling transformer is developed. A prototype was built and the aim of this paper is to study its behavior during all operation modes for which it is intended under grid conditions. It is shown that it does realize the voltage regulation function during normal operation mode as well as it is able to self-protect against grid fault conditions during fault operation.**

***Index Terms*—Short-circuit currents, transformer cores, voltage fluctuations**

I. Introduction

Voltage fluctuations in electrical grids are a major problem, liable for power quality decreases and economic losses [1]–[4]. Among all existing Flexible AC Transmission Systems (FACTS) [5] and custom power devices, the Dynamic Voltage Restorer (DVR) [6]–[9] is an effective solution to mitigate voltage sags and swells, and so to efficiently improve the power quality. The working principle is simple: a DVR compensates voltage fluctuations by injecting the proper amount of voltage in series with the supply voltage in order to keep the load voltage at the rated value [6]–[13].

A typical DVR is composed of a coupling transformer whose first winding is inserted in series in the electrical grid and whose second winding is connected to an energy storage unit through a Voltage Source Converter (VSC). However, as it is inserted in the electrical grid continuously, the protection of the VSC against high fault currents constitutes its weak point. Three approaches are usually used for the existing DVR to avoid damaging the VSC.

- The first approach consists in oversizing it. The drawback of this solution is that it is expensive as well as it increases the size of the converter [14].
- The second approach consists in inserting an electromechanical bypass in parallel with the coupling transformer in order to disconnect it from the electrical grid during the presence of a fault current. The drawback of this solution lies in the time response of this protection scheme, which is quite high (around 100 ms [10,11,15]).
- The third approach consists in using a specific control strategy for the VSC [16]–[20]. The drawback of this method is also the response time which is, at best, around one electrical period.

To improve the protection of the VSC, the proposed solution is based on a magnetic bypass directly integrated inside the magnetic core of the coupling transformer [21]. It is realized by the adding of a return leg to a standard transformer and the use of the virtual air gap principle [22,23] to modify the distribution of the magnetic flux according to the electrical grid conditions. The advantage of this solution lies in the fact that the response time of the device is instantaneous.

Up to now, the authors studied the operating principle of this device in fault operation with a single phase reduced-scale device [24]. The capacity of the magnetic bypass to limit the current in the winding connected to the VSC was validated by both Finite Element Analysis (FEA) and laboratory experiments. Nevertheless, due to the power limitation of this reduced-scale device, the tested fault current was only 1 A. Moreover, the voltage regulation function was not validated. Then, based on this result, the authors extrapolated the operation of such a device at industrial rated electrical values. The design procedure and rules of a prototype were detailed in [25].

The aim of this paper is twofold. Firstly, validate that the original function of a DVR, which is to operate as a voltage transformer under normal operation, is not impacted by the addition of the return leg. In particular, it is highlighted that it does not impact the harmonic content, i.e. the quality, of the electrical grid voltage. This is a key point since it shows that the proposed DVR does not affect the other loads and/or drives in the grid in which it is inserted. Secondly, show that the VSC is protected against fault current peaks up to three times its rated current.

II. Dynamic Voltage Restorer With the VSC Protected by a Magnetic Bypass

A. Coupling transformer with a magnetic bypass

The magnetic core of the coupling transformer of the DVR whose VSC is protected by a magnetic bypass is composed of two parts: a classical transformer part and a return leg, as shown in Fig. 1 [21,25]. The transformer part is exactly the same as the one of existing DVRs. The first winding is inserted

This work is supported by Electricité de France (EDF) Research and Development and by the MEDEE Program supervised by the French National Technological Research Cluster in Electrical Machine Efficiency Increase through the Région Hauts-de-France, France, the French Ministry and the European Funds (Fonds Européen de développement Économique Régional).

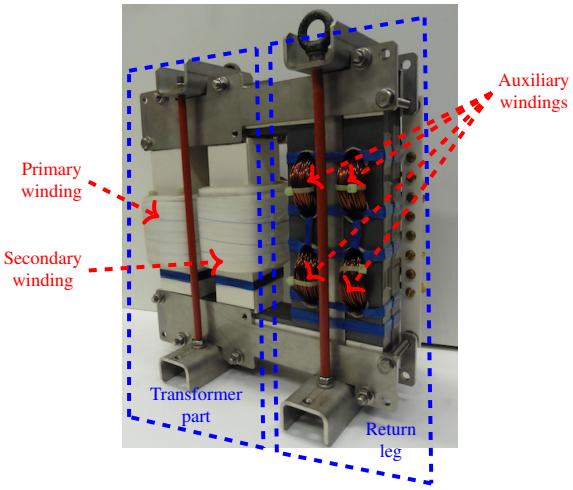

Fig. 1. Experimental device of the coupling transformer

TABLE I
CHARACTERISTICS OF THE LOW VOLTAGE COUPLING TRANSFORMER

Rated AC Voltage V_{sn}	23 V_{rms}
Rated AC Current I_{pn}	41 A_{rms}
Rated Power	1 kV A
Size of the magnetic circuit (Length×Width×Thickness)	30 cm × 30 cm × 4.8 cm
Magnetic sheets	PowerCore CGO135-35
Number of turns of the main windings	32
Number of turns of the auxiliaries windings	4×80

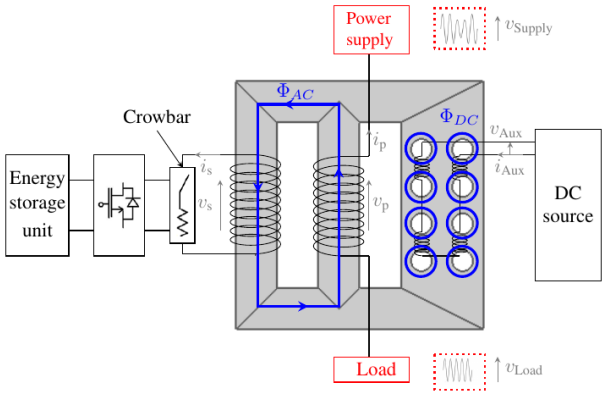

(a) Normal operation

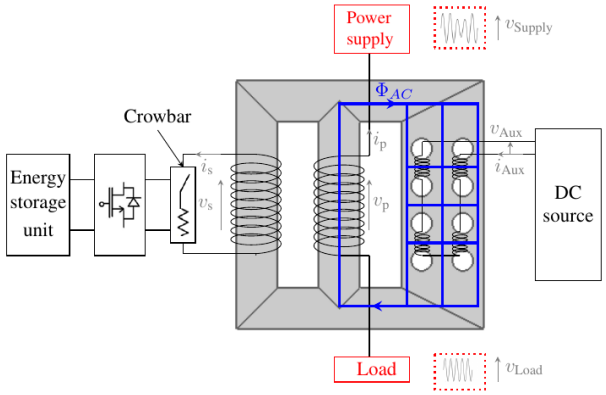

(b) Fault operation

Fig. 2. DVR working principle

in series in the electrical grid between a power supply and critical loads. The second winding is connected to an energy storage unit through a VSC to inject the appropriate voltage in case of an upstream electrical grid voltage fluctuation. The return leg, composed of four pairs of holes, aims to protect the VSC by deflecting the magnetic flux generated in the transformer part, from the leg connected to the VSC to the return leg, in fault operation. This magnetic bypass is based on the virtual air gap principle [22], i.e the local saturation of a magnetic core by auxiliary windings inserted in drilled holes and supplied by a DC source (chopper). Table I provides the characteristics of the prototype presented in Fig. 1.

In normal operation, the return leg is saturated by supplying the auxiliary windings with either a DC voltage or a DC current, denoted v_{Aux} and i_{Aux} respectively (Fig. 2a) [24]. That way, the voltage at the load terminals, denoted v_{load}, can be regulated to compensate electrical grid voltage fluctuations.

When a fault current is detected in the primary winding, the crowbar is closed (Fig. 2) and the device switches to fault operation mode. In fault operation, the AC magnetic flux generated by that fault current is higher than de DC magnetic flux generated by the auxiliary windings. Hence, it can circulate in the return leg instead of the leg connected to the VSC (Fig. 2b). So, in fault operation, the deflection of the AC magnetic flux in the return leg allows the magnetic bypass to act as a VSC electrical grid fault current protection scheme. In this operation mode, two strategies exist to supply the auxiliary windings:

1) keep i_{Aux} at the same value as in normal operation ;
2) cancel it.

The best strategy is the second one, i.e. set $i_{Aux} = 0$, since it makes the reluctance of the return leg lower. For this reason, the flux deflection is easier, allowing for a better protection of the DC source (battery + chopper) against voltage surges.

III. TEST BED AND EXPERIMENTAL PROTOCOL

A. Test bed

Experimental tests are made in laboratory in order to validate that the prototype is able to fulfill its function in both normal and fault operation under electrical grid conditions. The three-phase test bed is presented in Fig. 3. Each phase is composed as follows:

- the DVR itself ;
- an energy storage units ;
- a VSC ;
- an AC power supply ;
- a DC source ;
- a purely resistive load ;
- one phase of an induction motor.

The energy storage unit is composed of three 36 V batteries wired in parallel. The VSC is a voltage inverter and is connected to the secondary winding of the DVR. The AC power

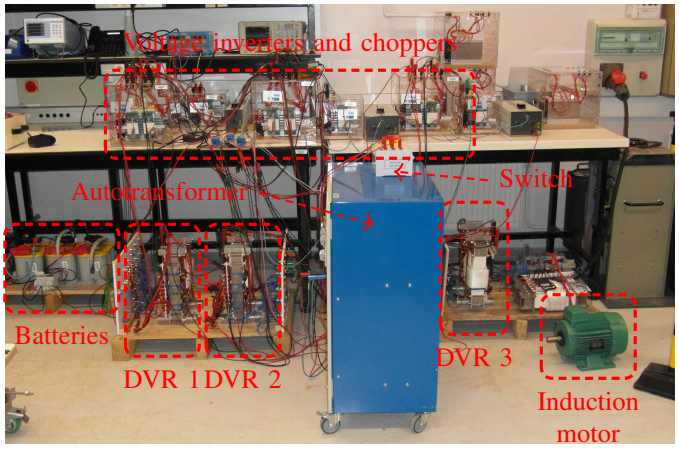

(a) Overview of the test bed

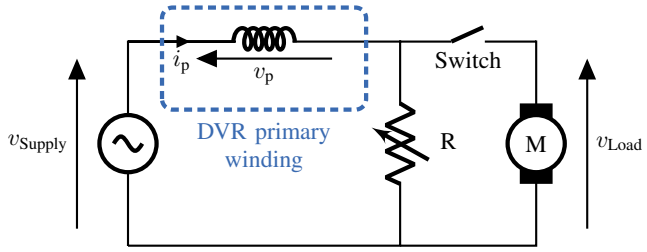

(b) Outline schematic of one phase of the test bed

Fig. 3. Experimental test bed

supply is a 400/230 V autotransformer and the DC source is a chopper.

The experimental protocol is different between normal and fault operation.

B. Experimental protocol: normal operation

The aim of the test performed in normal operation is to show the ability of the proposed DVR to regulate v_{Load} at its rated value for $v_{Supply} = v_{Load,rated} \pm 10\,\%$ with $v_{Load,rated} = 230\,V$. Hence, the chopper plays its role by supplying the auxiliary windings with a DC voltage in order to saturate the return leg. The load connected to the primary winding is purely resistive (the induction motor is not connected). Hence, the higher the resistance is, the higher the current i_p is, and then the lower the load voltage v_{Load} is. The crowbar is open so the voltage inverter connected to the secondary winding can play its role by injecting the appropriate voltage in order to compensate the voltage drop between v_{Supply} and v_{Load}. The test is performed for several resistance values.

C. Experimental protocol: fault operation

The aim of the test performed in fault operation is to show the ability of the device to protect the VSC from fault currents. For safety reasons, the fault current is simulated by the inrush current of an 11 kW induction motor. The test is performed as follows. First, the DVR runs in normal operation, as detailed in Section III-B, which means that the load voltage v_{Load} is regulated while the current is kept its rated value $I_{Aux} = 41\,A$.

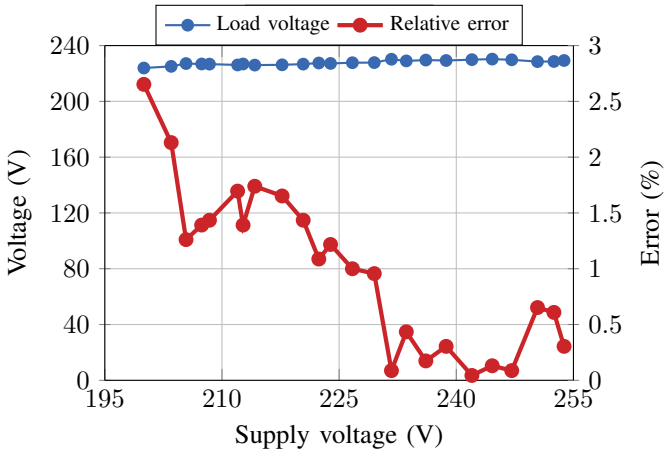

Fig. 4. Variation of regulated v_{Load} and relative error between v_{Load} and its rated value with respect to v_{Supply} during regulation

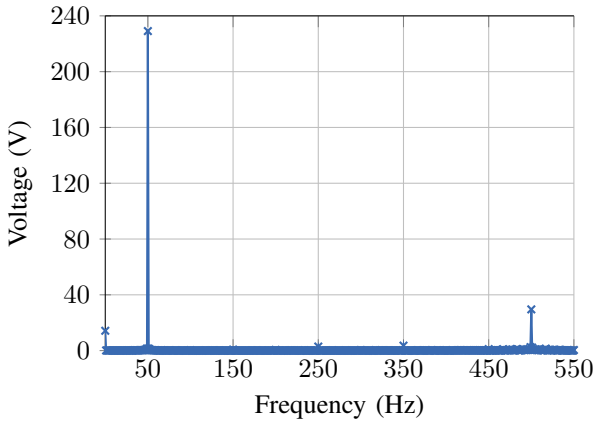

Fig. 5. Harmonic content of v_{Load} during regulation

Then, the induction motor is suddenly started by closing the switch (Fig. 3b), leading to a high current draw in the primary winding. This "fault current" is detected , the crowbar is closed and the VSC stops regulating. Then, as previously mentioned, i_{Aux} can be held at its rated value or cancelled. Both strategies are analyzed in the result Section. Finally, as the induction motor rotor speed increases, the current decreases, allowing for the VSC to start regulating again.

IV. Experimental Results

A. Normal operation: voltage regulation

Fig. 4 shows the value of the regulated v_{Load} for different values of v_{Supply}. It can be seen that the device is able to maintain v_{Load} at its rated value (230 V) no matter the value of v_{Supply}.

Since the auxiliary windings produce a DC magnetic flux, one could worry about the influence of the return leg on the waveform, and thus on the quality, of v_{Load}. Fig. 5 presents the harmonic content of v_{Load}. Only two peaks appear. The first one, located at 50 Hz, corresponds to the fundamental

frequency. The second one, located at 500 Hz, corresponds to the switching frequency of the VSC. This switching frequency might seem too low for a use of the device in an electrical grid. The reason for such a switching frequency is the use of simple Arduino Unos for the command of the voltage inverters. Hence, this point can easily be improved either by using another hardware, or by filtering. In any case, Fig. 5 highlights that the saturation of the return leg does not bring any additional harmonics to the voltage of the grid the proposed DVR is connected to.

B. Fault operation: protection of the VSC

As detailed in Section III-C, the test protocol consists in starting an 11 kW-induction motor such that the inrush current allows to safely simulate a fault current. As soon as this sudden current exceeds a critical value (set by the user), the fault detection flag is set to *high*, the VSC stops regulating v_{Load} and the crowbar is closed. Then, once the current drops below the aforementioned critical value, the fault detection flag is set to *low*, the crowbar is open and the VSC starting regulating v_{Load} again. The critical value for which the fault detection flag is switched is set to 55 A.

Fig. 6a, 6b and 6c presents the variation of i_{p} and i_{s} with respect to time during the whole process. For the sake of readability, the variation of the fault detection flag is also represented in these figures.

In order to evaluate the performances of the proposed DVR, as well as the two aforementioned strategies about i_{Aux}, i.e. keep it at its rated value or cancel it, a reference test if performed. It consists in using a version of the DVR without the return leg. In other words, in this case, the VSC is not protected against fault current since the flux generated by this latter can not be deflected. The results of that test, still following the protocol detailed in Section III-C are presented in Fig. 6a. In this figure, it can be seen that with such a device, which consists in nothing more than a one-phase transformer (Fig. 1), i_{s} follows i_{p}.

Fig. 6b and 6c present the results obtained with the DVR including the return leg (Fig. 1 and 2) with $i_{\text{Aux}} = 7\,\text{A}$ and $i_{\text{Aux}} = 0\,\text{A}$ respectively. In can be seen that, in both cases, i_{s} is clipped until the fault detection flag comes back to *low*. It can be noted that even for $i_{\text{p}} = 155\,\text{A}$, the maximum value of i_{s} is limited to a value below 60 A.

The difference between the two strategies lies in the value of this limit, which is lower in the case where $i_{\text{Aux}} = 0\,\text{A}$. It can be particularly noted on the second period of i_{s} during fault operation.

In any case, Fig. 6 highlights that the proposed DVR is able to protect the VSC from fault current.

C. Response times

The major issue about all the methods found in the literature to protect the VSC of DVRs against fault currents is about the response time. No matter the method [10,11,15]–[20], this response time is always higher than 10 ms.

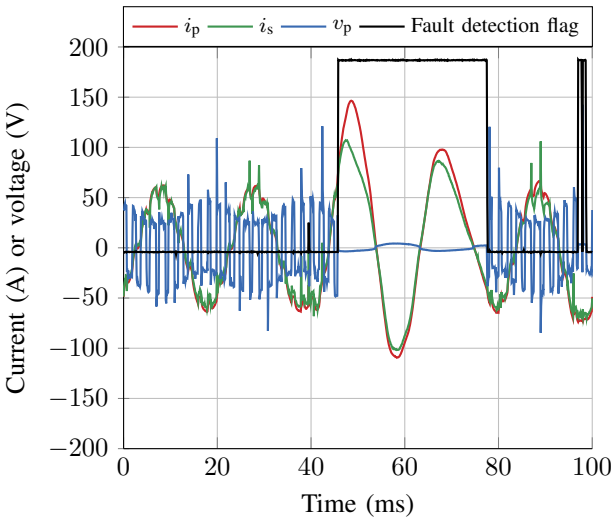

(a) DVR with unmouted return leg

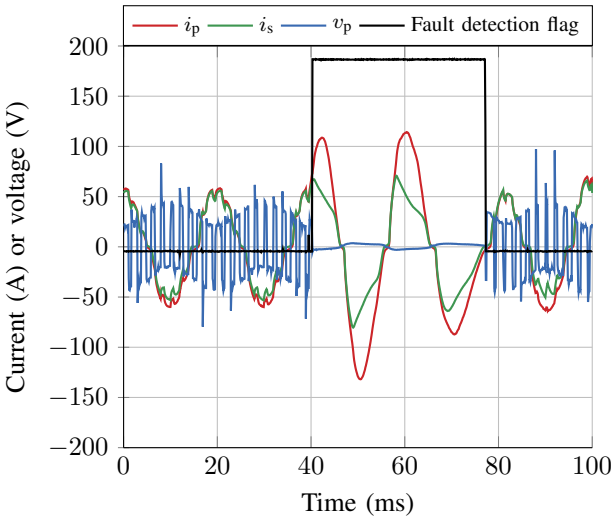

(b) i_{Aux} is maintained at 7 A during both normal and fault operation

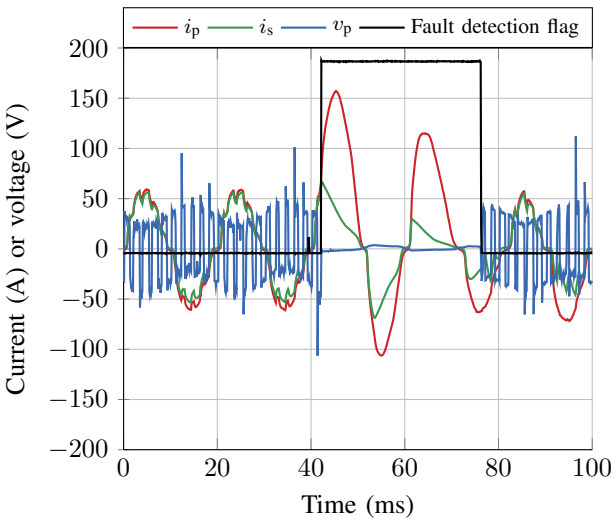

(c) i_{Aux} is cancelled during fault operation

Fig. 6. Variation of i_{p}, i_{s} and v_{Supply} during the motor starting

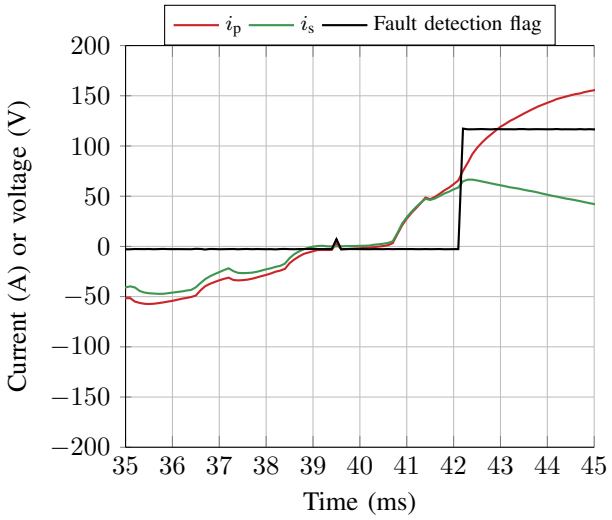

Fig. 7. Variation of i_p and i_s during the motor starting - response time of the DVR

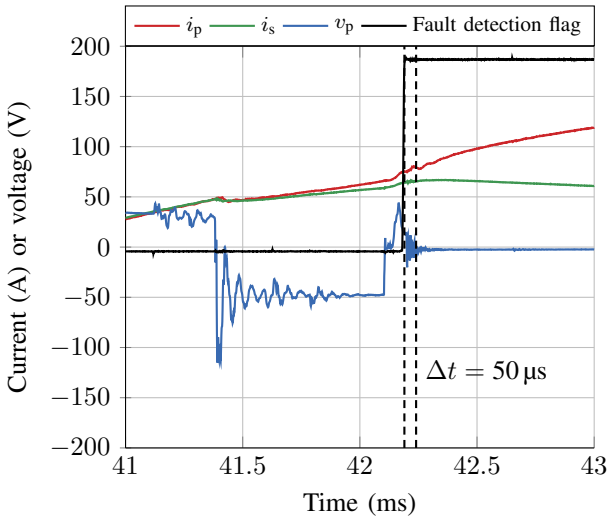

Fig. 8. Variation of i_p and i_s during the motor starting - response time of the command of the VSC

Fig. 6 clearly shows that the response time of the proposed DVR is under that amount of time. For a better investigation, Fig. 7 shows the variations of i_p and i_s, zoomed on the fault detection time. Even with this reference time, it seems that proposed DVR ensures an instant response regarding the clipping of i_s.

The command response time is also to consider. It is shown in Fig. 8 and is around 50 µs, which is actually the hardware limit of the Arduino Uno.

D. Losses in the return leg and the auxiliary windings

The main drawback of the device lies in the fact that the return leg needs to be permanently saturated during normal operation in order for the DVR to regulate v_{Load}. This excitation leads to losses.

Core losses are caused by hysteresis and eddy current effects. Nevetheless, as detailed in Section II, the auxiliary windings are fed with a DC current. For this reason, the magnetic flux generated in the return leg is not responsible for any additional core losses.

As for the Joule losses, the results presented in Section IV are obtained with $i_{Aux} = 7\,A$. The resistance of the auxiliary windings is $1\,\Omega$, which leads to an amount of Joule losses of 49 W for a 1 kV A DVR. The quantity to focus on is the magnetomotive force generated by the auxiliary windings, i.e. the ampere-turns. Then, two strategies can be followed in order to lower the Joule losses while keeping the magnetomotive force at the same value:

- lower the resistance of the auxiliary windings by either lowering the number of turns or increasing the section of the wire.
- lower i_{Aux} ;

Due to geometrical constraints, detailed in [25], the geometry of the return leg can not be modified. Hence, the holes in which the auxiliary windings are wound can not be increased. For this reason, lowering the number of turns or increasing the section of the wire is not an option.

Lowering i_{Aux} is possible. The only constraint is to keep the magnetomotive force generated by the auxiliary windings at least equal to the one generated by the primary windings during normal operation such that the local saturation of the return leg is not disturbed. According to Table I, the minimum value for i_{Aux} is 3 A. Additional tests with $i_{Aux} = 5\,A$ where performed and showed that, at this value, the return leg start suffering from a slight desaturation. In this case, it behaves as a leaking inductance and start influencing the regulation process.

V. Conclusion

In this paper, a prototype of a DVR with electronics protected from fault currents under electrical conditions was presented. The device was experimentally tested in both normal and fault operations. It was highlighted that it is able to perform a regulation function as well as to protect the VSC from fault currents. Some parameters that might influence the behavior of the proposed device are still to be investigated, such as the grade of the magnetic steel used to build the return leg.

References

[1] N. Edomah, "Effects of voltage sags, swell and other disturbances on electrical equipment and their economic implications," in *CIRED 2009 - 20th International Conference and Exhibition on Electricity Distribution*, 2009, pp. 1–4.

[2] Z. Klaic, D. Sipl, and S. Nikolovski, "Economic impact of power quality disturbances," in *CIRED 2013 - 22nd International Conference and Exhibition on Electricity Distribution*, 2013, pp. 1123–1123.

[3] J. Milanovic, "Economic impact of power quality disturbances on customers and utilities," in *IET Conference on Power in Unity: a Whole System Approach*. Institution of Engineering and Technology, 2013, pp. 4.06–4.06.

[4] S. Elphick, P. Ciufo, V. Smith, and S. Perera, "Summary of the economic impacts of power quality on consumers," in *2015 Australasian Universities Power Engineering Conference (AUPEC)*, Sep. 2015, pp. 1–6.

[5] S. A. Rahman, H. Maleki, S. Mohan, R. K. Varma, and W. H. Litzenberger, "Bibliography of FACTS 2013-2014: IEEE working group report," in *2015 IEEE Power & Energy Society General Meeting*, Jul. 2015, pp. 1–5.

[6] J. Praveen, P. Bishnu, S. Muni, and H. Makthal, "Review of dynamic voltage restorer for power quality improvement," in *30th Annual Conference of IEEE Industrial Electronics Society (IECON)*, vol. 1, 2004, pp. 749–754.

[7] J. Nielsen and F. Blaabjerg, "A Detailed Comparison of System Topologies for Dynamic Voltage Restorers," *IEEE Transactions on Industry Applications*, vol. 41, no. 5, pp. 1272–1280, Sep. 2005.

[8] M. A. Bhaskar, S. Dash, C. Subramani, M. J. Kumar, P. Giresh, and M. V. Kumar, "Voltage Quality Improvement Using DVR," in *2010 International Conference on Recent Trends in Information, Telecommunication and Computing*, Mar. 2010, pp. 378–380.

[9] A. K. Sadigh and K. M. Smedley, "Review of voltage compensation methods in dynamic voltage restorer (DVR)," in *2012 IEEE Power and Energy Society General Meeting*. IEEE, Jul. 2012, pp. 1–8.

[10] A. Kara, P. Dahler, D. Amhof, and H. Gruning, "Power supply quality improvement with a dynamic voltage restorer (DVR)," in *30th Annual Applied Power Electronics Conference and Exposition (APEC)*, vol. 2, 1998, pp. 986–993.

[11] N. Woodley, L. Morgan, and A. Sundaram, "Experience with an inverter-based dynamic voltage restorer," *IEEE Transactions on Power Delivery*, vol. 14, no. 3, pp. 1181–1186, Jul. 1999.

[12] A. M. Rauf and V. Khadkikar, "An Enhanced Voltage Sag Compensation Scheme for Dynamic Voltage Restorer," *IEEE Transactions on Industrial Electronics*, vol. 62, no. 5, pp. 2683–2692, May 2015.

[13] J. M. Ramirez, P. Garcia-Vite, J. M. Lozano, and F. Mancilla-David, "Dynamic voltage restorers based on AC-AC topologies," in *2012 IEEE Power and Energy Society General Meeting*, Jul. 2012, pp. 1–7.

[14] T. Jimichi, H. Fujita, and H. Akagi, "Design and Experimentation of a Dynamic Voltage Restorer Capable of Significantly Reducing an Energy-Storage Element," *IEEE Transactions on Industry Applications*, vol. 44, no. 3, pp. 817–825, 2008.

[15] J. Magnusson, J. A. Martinez-Velasco, A. Bissal, G. Engdahl, and L. Liljestrand, "Optimal design of a medium voltage hybrid fault current limiter," in *IEEE International Energy Conference (ENERGYCON)*, 2014, pp. 431–438.

[16] Y. W. Li, D. M. Vilathgamuwa, P. C. Loh, and F. Blaabjerg, "A Dual-Functional Medium Voltage Level DVR to Limit Downstream Fault Currents," *IEEE Transactions on Power Electronics*, vol. 22, no. 4, pp. 1330–1340, 2007.

[17] S. Choi, T. Wang, and D. M. Vilathgamuwa, "A Series Compensator With Fault Current Limiting Function," *IEEE Transactions on Power Delivery*, vol. 20, no. 3, pp. 2248–2256, Jul. 2005.

[18] F. Badrkhani Ajaei, S. Farhangi, and R. Iravani, "Fault Current Interruption by the Dynamic Voltage Restorer," *IEEE Transactions on Power Delivery*, vol. 28, no. 2, pp. 903–910, 2013.

[19] Z. Shuai, P. Yao, Z. J. Shen, C. Tu, F. Jiang, and Y. Cheng, "Design Considerations of a Fault Current Limiting Dynamic Voltage Restorer (FCL-DVR)," *IEEE Transactions on Smart Grid*, vol. 6, no. 1, pp. 14–25, 2015.

[20] H. Nourmohamadi, S. I. Bektas, S. H. Hosseini, E. Babaei, and M. Sabahi, "A conventional dynamic voltage restorer with fault current limiting capability," *Procedia Computer Science*, vol. 120, pp. 750–757, 2017.

[21] P. Guuinic, J.-F. Brudny, V. Costan, and M. Dessoude, "Series voltage regulator with electronics protected against short-circuits by magnetic circuit-based decoupling using holes and windows," WO Patent WO2 012 126 884 A3, 2013, wO 2012/126884.

[22] V. Molcrette, J.-L. Kotny, J.-P. Swan, and J.-F. Brudny, "Reduction of inrush current in single-phase transformer using virtual air gap technique," *IEEE Transactions on Magnetics*, vol. 34, no. 4, pp. 1192–1194, jul 1998.

[23] J.-F. Brudny, G. Parent, and I. Naceur, "Characterization and Modeling of a Virtual Air Gap by Means of a Reluctance Network," *IEEE Transactions on Magnetics*, vol. 53, no. 7, pp. 1–7, Jul. 2017.

[24] V. Majchrzak, G. Parent, J.-F. Brudny, V. Costan, and P. Guuinic, "Coupling transformer with a virtual air gap for the protection of dynamic voltage restorers," in *40th Annual Conference of the IEEE Industrial Electronics Society (IECON)*, 2014, pp. 462–468.

[25] ——, "Design of a Coupling Transformer With a Virtual Air Gap for Dynamic Voltage Restorers," *IEEE Transactions on Magnetics*, vol. 52, no. 7, pp. 1–4, Jul. 2016.